

# Characterization of *CDH3*-Related Congenital Hypotrichosis With Juvenile Macular Dystrophy

Sarah Hull, MA, FRCOphth; Gavin Arno, PhD; Anthony G. Robson, MSc, PhD; Suzanne Broadgate, PhD; Vincent Plagnol, PhD; Martin McKibbin, FRCOphth; Stephanie Halford, PhD; Michel Michaelides, MD(Res), FRCOphth; Graham E. Holder, MSc, PhD; Anthony T. Moore, MA, FRCOphth; Kamron N. Khan, PhD, FRCOphth; Andrew R. Webster, MD(Res), FRCOphth

**IMPORTANCE** Congenital hypotrichosis with juvenile macular dystrophy (HJMD) is a rare disorder presenting in childhood and adolescence with central visual disturbance and sparse scalp hair. Reported retinal imaging is lacking, and whether the condition is progressive remains unclear.

**OBJECTIVE** To investigate a series of patients with HJMD due to biallelic mutations in *CDH3* and thereby characterize the disorder.


**DESIGN, SETTING, AND PARTICIPANTS** Ten patients from 10 families underwent detailed clinical assessment, including serial retinal imaging and electrophysiologic evaluation, at Moorfields Eye Hospital, St James's University Hospital, and Calderdale Royal Infirmary. Patients ranged in age from 3 to 17 years at onset and 5 to 57 years at last assessment. The molecular genetic investigation included bidirectional Sanger sequencing of all exons and intron-exon boundaries of *CDH3* and whole-exome sequencing in 2 patients. The study was conducted from June 5, 2013, to January 15, 2016, with final follow-up completed on December 15, 2015.

**MAIN OUTCOMES AND MEASURES** Results of clinical assessment and molecular genetic testing.

**RESULTS** All 10 patients (7 male and 3 female) presented with central visual disturbance in childhood and had lifelong sparse scalp hair with normal facial hair. Fundus examination revealed chorioretinal atrophy of the posterior pole contiguous with the disc in all but 1 patient that was associated with marked loss of autofluorescence on fundus autofluorescence imaging. Optical coherence tomography (OCT) demonstrated variable degrees of atrophy of the outer retina, retinal pigment epithelium, and choroid, with outer retinal tubulations frequently observed. One patient had mild disruption of the inner segment ellipsoid band on OCT and additional mild digit abnormalities. Electrophysiologic evaluation in 5 patients demonstrated macular dysfunction with additional mild, generalized retinal dysfunction in 2 patients. Eight patients had more than 1 evaluation; of these, 5 patients showed deterioration of visual acuity over time, 1 patient remained stable, and 2 patients had severe visual loss at presentation that precluded assessment of visual deterioration. The area of atrophy did not progress with time, but retinal thickness decreased on OCT. Electrophysiologic evaluation in 1 patient found deterioration of macular function after 13 years of follow-up, but the mild, generalized photoreceptor dysfunction remained stable. Biallelic mutations were identified in all patients, including 6 novel mutations.

**CONCLUSIONS AND RELEVANCE** These results suggest that *CDH3*-related disease is characterized by a childhood-onset, progressive chorioretinal atrophy confined to the posterior pole. The disease is readily distinguished from other juvenile macular dystrophies by the universally thin and sparse scalp hair. Patients may have additional limb abnormalities.

JAMA Ophthalmol. 2016;134(9):992-1000. doi:10.1001/jamaophthalmol.2016.2089  
Published online July 7, 2016.

 Supplemental content at [jamaophthalmology.com](http://jamaophthalmology.com)

**Author Affiliations:** UCL (University College of London) Institute of Ophthalmology, London, England (Hull, Arno, Robson, Michaelides, Holder, Moore, Khan, Webster); Moorfields Eye Hospital, London, England (Hull, Arno, Robson, Michaelides, Holder, Moore, Khan, Webster); Nuffield Laboratory of Ophthalmology, Nuffield Department of Clinical Neuroscience, University of Oxford, Oxford, England (Broadgate, Halford); UCL Genetics Institute, London, England (Plagnol); Department of Ophthalmology, St James's University Hospital, Leeds, England (McKibbin, Khan); Department of Ophthalmology, University of California, San Francisco, Medical Center (Moore).

**Corresponding Author:** Andrew R. Webster, MD(Res), FRCOphth, UCL Institute of Ophthalmology, 11-43 Bath St, London EC1V 9EL, England ([andrew.webster@ucl.ac.uk](mailto:andrew.webster@ucl.ac.uk)).

First described in 2 brothers in 1935, congenital hypotrichosis with juvenile macular dystrophy (HJMD [OMIM 601553]) presents in childhood with central visual loss and associated abnormality of the scalp hair.<sup>1</sup> Congenital HJMD is a rare, recessively inherited disorder reported to date in a total of 21 families with molecular confirmation and 15 different causative mutations.<sup>2-12</sup> The disease is caused by biallelic loss of function mutations in the *CDH3* gene (OMIM 114021), which encodes P-cadherin, a regulator of hair, retinal pigment epithelium (RPE), and limb development.<sup>2,7</sup> Ectodermal dysplasia, ectrodactyly, and macular dystrophy syndrome (EEMS [OMIM 225280]) constitute an allelic disorder also associated with biallelic *CDH3* mutations.<sup>13</sup> The phenotype for EEMS is variable, with macular dystrophy; ectodermal involvement that includes hypotrichosis, nail dysplasia, and partial anodontia; and limb defects that include syndactyly (joined digits), campyloactyly (bent digits), or ectrodactyly (missing phalanges that, when most severe, has a claw-hand appearance). Only 6 families with molecular confirmation have been reported in the literature, with 5 additional pathogenic mutations in *CDH3* identified.<sup>6,7,13,14</sup>

Apart from a series of 7 families that focused on electrophysiologic findings, the previous descriptions of *CDH3*-related macular dystrophy contain limited retinal imaging and electrophysiologic data.<sup>15,16</sup> This study reports the results of detailed phenotyping, including serial imaging and electrophysiologic evaluation, in 10 patients with biallelic *CDH3* mutations and describes 6 novel mutations.

## Methods

### Clinical Assessment

Patients for this study were ascertained from Moorfields Eye Hospital (London, England), St James's University Hospital (Leeds, England), and Calderdale Royal Infirmary (Halifax, England) from June 5, 2013, to January 15, 2016. The study protocol adhered to the tenets of the Declaration of Helsinki<sup>17</sup> and received approval from the local ethics committees. Written informed consent was obtained from all participants or parents of children before their inclusion in this study.

Each patient underwent a full clinical examination, including visual acuity (VA) and dilated fundus examination. Retinal fundus imaging was obtained by 35° color fundus photography (Topcon Great Britain Ltd), 30° or 55° fundus autofluorescence (FAF) imaging (Spectralis; Heidelberg Engineering Ltd), and optical coherence tomography (OCT) (Stratus [Carl Zeiss Meditec Inc] or Spectralis). Serial imaging was available for 9 eyes of 5 patients (patients 3, 5, 7, 8, and 10). The thickness of the Early Treatment Diabetic Retinopathy Study central subfield region was measured using an automated viewing module (Heidelberg Spectralis viewing module, version 6.3.4.0), with the RPE basement membrane and the internal limiting membrane layers checked for accuracy in each OCT section and manually corrected if necessary. The size of the atrophic region was mapped for each FAF image, with the region first highlighted using Adobe Photoshop Elements (ver-

### Key Points

**Question** What can a detailed phenotyping study of molecularly characterized patients with *CDH3*-related macular dystrophy reveal about the disease presentation and progression?

**Findings** This case series of 10 patients identified universal childhood-onset thin scalp hair in conjunction with predominant macular dysfunction. The retinal dystrophy appeared to be centrally progressive with preserved peripheral retinal function.

**Meaning** These data suggest that children presenting with macular dystrophy can be diagnosed as having *CDH3*-related disease based on examination of the scalp. The likely prognosis indicates preservation of peripheral vision.

sion 14; Adobe Systems Incorporated) and the area then calculated using color-measuring macros (Threshold Color plug-in in Image J; National Institutes of Health). We assessed only those images in which the atrophic region border could be clearly delineated, which was possible for patients 5 and 7. Full-field and pattern electroretinography (ERG and PERG, respectively) were obtained in 5 patients using gold foil electrodes, which incorporated the International Society for Clinical Electrophysiology of Vision standards, with electro-oculography (EOG) studies performed in 2 patients.<sup>18,19</sup>

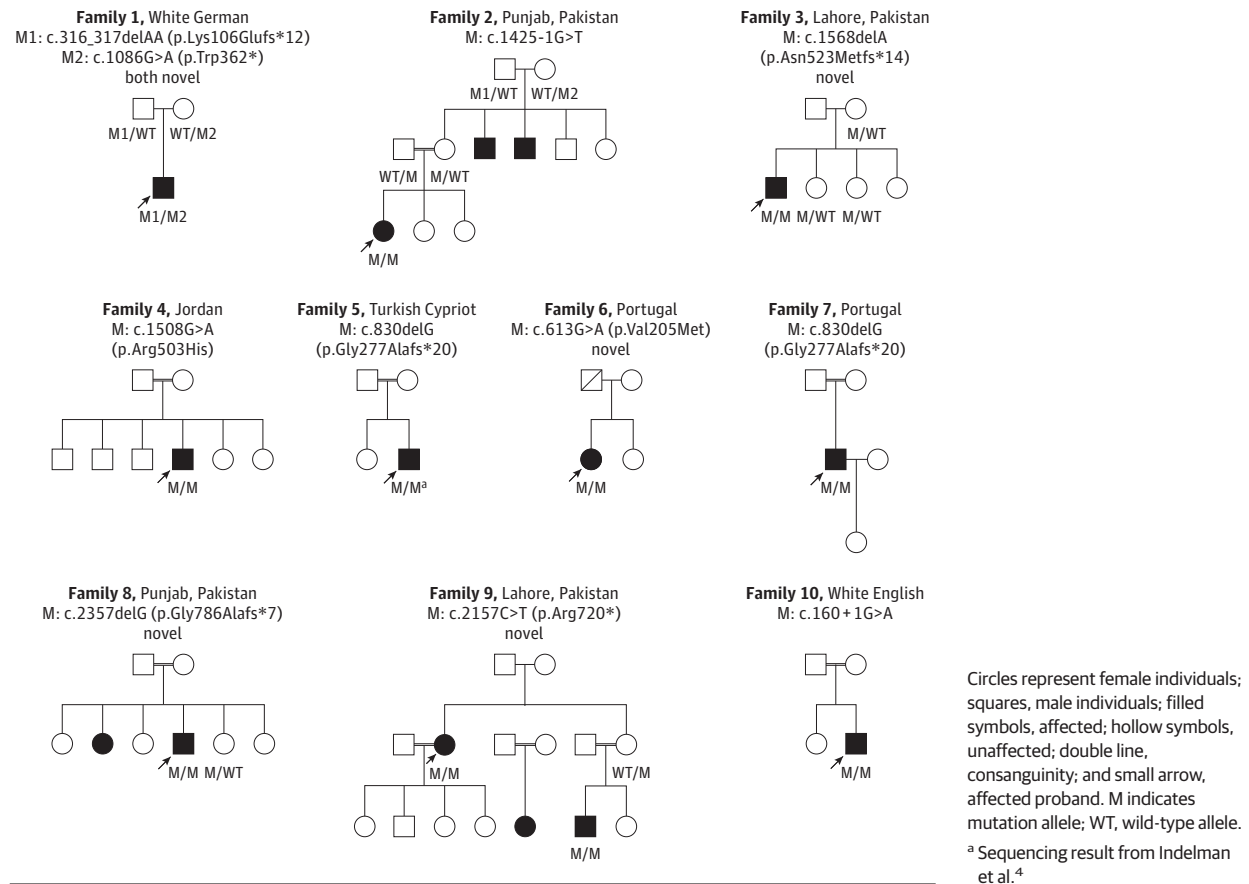
### Molecular Biological Assessment

Patient 3 had results of a previous molecular evaluation available from elsewhere.<sup>4</sup> Patient 1 had undergone targeted-capture, next-generation sequencing of a macular dystrophy gene panel consisting of *ABCA4*, *BEST1*, *CIQTNF5*, *CDH3*, *CLN3*, *CNGB3*, *CRB1*, *ELOVL4*, *FSCN2*, *IMPG1*, *PROM1*, *PRPH2*, *RDH12*, *RP11*, *RPGR*, *TIMP3*, and *TTL5* (Centre for Genomics and Transcriptomics).<sup>20</sup> Patients 3 and 8 underwent whole-exome sequencing, with Sanger sequencing confirmation and family segregation subsequently performed. Whole-exome sequencing was performed at AROS Applied Biotechnology using a solution-phase 38-Mb exome capture (SureSelect Human All Exon Kit; Agilent Technologies Inc) and a sequencer (HiSeq 2000; Illumina Inc). Reads were aligned to the hg19 human reference sequence using Novoalign (version 2.05; Novocraft). The ANNOVAR tool (Openbioinformatics.org) was used to annotate single-nucleotide polymorphisms and small insertions and deletions.

The mutations in the remaining patients were identified by Sanger sequencing of all exons and exon-intron boundaries of *CDH3*. We amplified DNA using specifically designed primers by polymerase chain reaction, and the resulting fragments were sequenced using standard protocols (eTable 1 in the Supplement). Segregation was performed in available family members.

Mutation nomenclature was assigned in accordance with GenBank NM\_001793.4 with nucleotide position 1 corresponding to the A of the ATG translation initiation codon. We identified variants as novel if not previously reported in the literature and if absent from dbSNP (<http://www.ncbi.nlm.nih.gov/projects/SNP/>); the National Heart, Lung, and Blood Institute GO Exome Sequencing Project (<https://esp.gs.washington.edu>

Figure 1. Pedigrees of 10 Families With Mutation Segregation



/drupal/); the 1000 Genomes Project (<http://www.1000genomes.org/>); and the Exome Aggregation Consortium (<http://exac.broadinstitute.org>), all accessed on January 25, 2016. The likely pathogenicity of missense variants was assessed using the predictive algorithms of SIFT (Sorting Intolerant From Tolerant) (<http://sift.jcvi.org>) and PolyPhen2 (<http://genetics.bwh.harvard.edu/pph2>); the conservation of the residues throughout the species was analyzed using Clustal Omega (<http://www.ebi.ac.uk/Tools/msa/clustalo/>) with identification of protein sequences from Ensembl (<http://ensembl.org/index.html>). Final follow-up was completed on December 15, 2015, and data were analyzed from October 30, 2015, to January 25, 2016.

**Results**

Ten patients (7 male and 3 female) from 10 families underwent investigation. Eight families were consanguineous (Figure 1). The clinical data are summarized in the Table. Most of the patients presented in the first decade of life with reduced central vision; the oldest presentation was at 17 years of age. Visual acuity was reduced in all patients at presentation, and at last review, deterioration was documented in 5 patients (range of review, 1-8 years). The mean age at last review was 27.2 (median, 24.5; range, 5-57) years, with VA ranging from 0.18 logMAR (Snellen, 20/30) to hand move-

ments. The oldest patients had a VA of 1.0 logMAR (Snellen, 20/200) or worse in their better-seeing eye, indicating severe sight impairment. The best VA was in patient 7, with 0.18 logMAR (Snellen, 20/30) OU at age 31 years. Four patients reported subjective deterioration of central vision. Only patient 4 reported nyctalopia. Nystagmus was not reported in any patient.

Fundus abnormalities consisted of variable degrees of atrophy of the retina, RPE, and choroid in the posterior pole, which in all but the youngest patient extended nasally to the disc (Figure 2 and eFigure 1 in the Supplement). The atrophy in 7 patients extended outside the arcades. Patient 1 had very mild macular atrophy of the outer retina only, whereas patients 9 and 10 had severe chorioretinal atrophy with exposed sclera. Variable degrees of hyperpigmented spots or clumps in the macula were evident in all patients.

Serial imaging (available in 5 patients) demonstrated increasing hyperpigmentation over time in 3 patients (demonstrated in Figure 2 for patient 7). Fundus autofluorescence imaging demonstrated confluent hypoautofluorescence in areas of atrophy with a surrounding ring of relatively increased autofluorescence in 6 of the 7 patients with FAF results available. A speckled hypoautofluorescence was present within the area of confluent atrophy in patients 5 and 8 (Figure 2). Patient 7 had small refractile deposits in both maculae.

Table. Clinical Summary

Patient No./ Family No./Variant	Age, y		VA, logMAR (Snellen)		Latest Refractive Error, D	Color Vision (Age, y)	Age at Last Electrophysiologic Evaluation, y/ Key Findings
	Onset	At Last Review (Duration)	Presenting	Final			
Patient 1/NA/c.316_317delAA (p.Lys106Glufs*12) and c.1086G>A (p.Trp362*)	3-4	5 (1)	OU, 0.32 (20/40)	OU, 0.63 (20/80)	OD, +8.50/-2.25 × 112 OS, +9.00/-1.75 × 70	Not performed	Not performed
Patient 2/NA/c.1425-1G>T	6	11 (2)	OD, 0.5 (20/63) OS, 0.8 (20/125)	OD, 0.6 (20/80) OS, CF	Not performed	Ishihara OU, 1/17 (10)	Not performed
Patient 3/GC18250/ c.1568delA (p.Asn523Metfs*14)	11	19 (6)	OU, 0.4 (20/50)	OD, 0.80 (20/125) OS, CF	OD, 0/-2.50 × 177 OS, -0.25/-2.25 × 162	Ishihara OD, 5/17 OS, 6/17 (13)	14/ Subnormal PERG P50 Normal ERGs Normal EOG
Patient 4/GC19726/ c.1508G>A(p.Arg503His)	4-5	20 (0)	OD, 1.0 (20/200) OS, 1.2 (20/320)	NA	Not performed	Ishihara OU, 1/17 (20)	20/Undetectable PERG Subnormal rod and subnormal and mildly delayed cone ERGs
Patient 5/GC20690/ c.830delG (p.Gly277Alafs*20)	5-6	24 (8)	OU, 0.30 (20/40)	OD, 0.80 (20/125) OS, 0.30 (20/40)	OD, +0.50/-2.00 × 5 OS, emmetropic	HRR Medium red/green defect, blue/yellow normal (22)	22/Undetectable PERG Mildly subnormal rod ERGs OD Other ERGs normal OU Normal EOG
Patient 6/GC22774/ c.613G>A/(p.Val205Met)	4	25	OD, 1.0 (20/200) OS, 1.2 (20/320)	NA	Myopic	Ishihara OD, 3/21 OS, 0/21 (25)	Not performed
Patient 7/GC18293/ c.830delG (p.Gly277Alafs*20)	8-9	31 (20)	OU, 0.18 (20/30)	OU, 0.18 (20/30)	OD, -1.00/-1.00 × 170 OS, -1.00/-0.50 × 60	Ishihara OD, 15/17 OS, 12/17 (28)	18/Markedly subnormal PERG P50 Subnormal rod ERGs and subnormal and delayed cone ERGs 27/Undetectable PERG; stable ERGs
Patient 8/GC19948/ c.2357delG (p.Gly786Alafs*7)	17	36 (3)	OD, 0.6 (20/80) OS, 1.2 (20/320)	OD, 0.84 (20/125) OS, 1.20 (20/320)	OD, -0.50/-0.50 × 40 OS, +0.50/-2.50 × 180	Ishihara OU, 1/17 (33)	33/Undetectable PERG Rod and cone ERGs normal OD Marginally subnormal OS due to eye closure
Patient 9/NA/c.2157C>T (p.Arg720*)	<10	44 (3)	OU, HM	OU, HM	Not performed	Not performed	Not performed
Patient 10/GC18996/c.160 + 1G>A	10	57 (7)	OU, 1.3 (20/400)	OU, 1.20 (20/320)	Not performed	HRR OU, no plates seen (54)	Not performed

Abbreviations: CF, counting fingers; D, diopter; EOG, electro-oculography; ERG, electroretinogram; HM, hand movements; HRR, Hardy, Rand and Rittler Pseudoisochromatic Plate test; NA, not applicable; PERG, pattern electroretinogram; VA, visual acuity.

In the 9 patients with OCT results available, variable degrees of atrophy were noted. In patient 1, only mild disturbance of the inner segment ellipsoid band was observed; patient 10 showed extensive atrophy of the retina, RPE, and choroid in addition to a serous retinal detachment over the atrophic area in the left eye (Figure 2). In the remaining 7 patients, outer retinal and RPE atrophy was present, with partial preservation of the inner segment ellipsoid band at the fovea in patient 7. Seven patients had outer retinal tubulations, and patient 5 in addition had intraretinal cysts in the outer nuclear layer. The overall size of the atrophic region did not appear to increase with time based on measurements in 2 patients only. However, retinal thickness within the atrophic region decreased with time in all 5 patients undergoing measurement for 2 to 10 years (eFigure 2 in the Supplement).

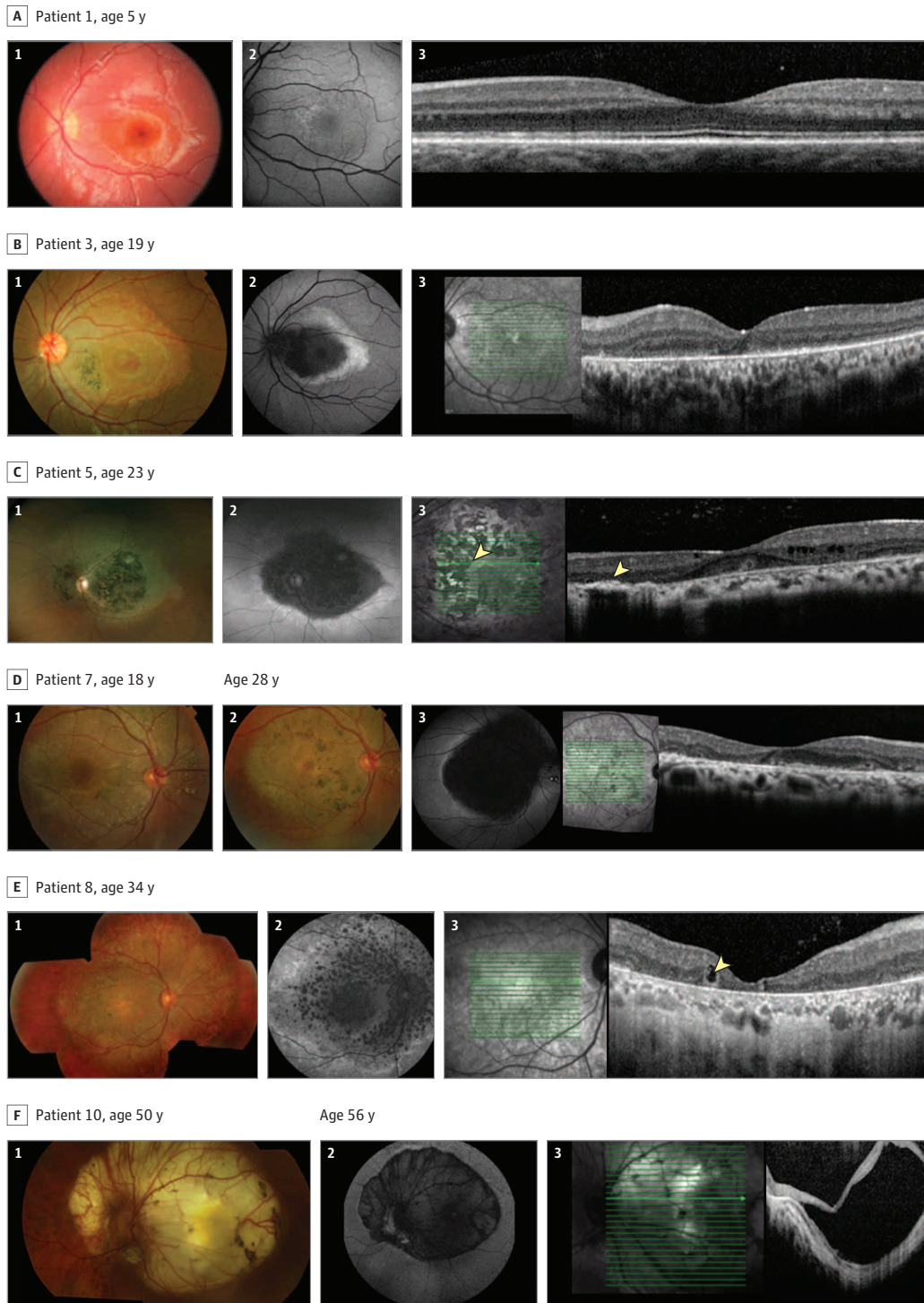
Electrophysiologic evaluation demonstrated undetectable PERG in 3 of the 5 patients with test results, consistent with severe macular dysfunction (Figure 3 and eFigure 3 in the Supplement). A subnormal PERG P50 component was

found in patient 3 at age 14 years in keeping with moderate macular dysfunction. In patient 7, the PERG was markedly subnormal at age 18 years and was undetectable at examination 9 years later (Figure 3). Bilateral full-field ERG abnormalities were present in patients 4 and 7, indicating mild, generalized rod and cone dysfunction (Figure 3). Marginal reductions were found in the rod-mediated ERGs in the right eye of patient 5 and rod and cone ERGs in the left eye of patient 8, but these were likely consequent on eye closure. The full-field ERGs in patient 7 showed no significant change at retesting after 9 years. Patients 3 and 5 underwent EOG studies with normal findings.

Systemically, all patients had thin scalp hair from at least early childhood, with normal hair elsewhere, including eyebrows (eFigure 4 in the Supplement). Patient 1 had mild webbing between the second and third digits of his left hand and campylodactyly of his feet, most apparent in the second digits of each foot. All other patients had normal limbs.

Molecular genetic testing identified biallelic mutations in *CDH3* in all 10 patients, including 5 novel premature

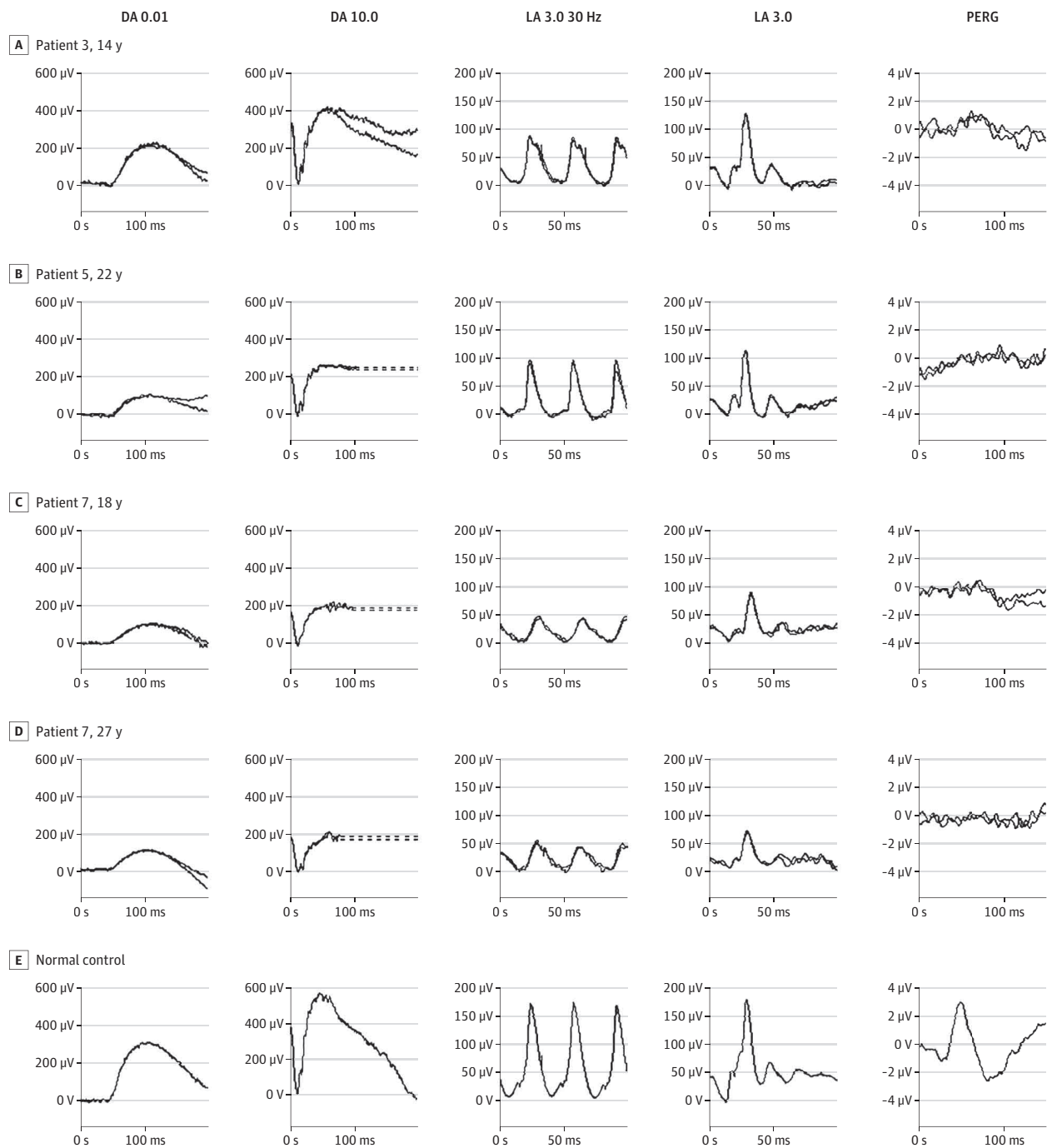
Figure 2. Retinal Imaging in 6 Patients



Color fundus photographs (1), fundus autofluorescence (FAF) imaging (2), and optical coherence tomography (OCT) (3) are shown for each patient. Patient 1 had mild pigment change on color fundus photography; increased autofluorescence nasally indicating loss of photoreceptor outer segments on FAF imaging; and disruption of the inner segment ellipsoid band on OCT. For all other patients, color fundus photography showed posterior pole atrophy encompassing the optic disc, most marked in patient 10, with exposed sclera and hyperpigmented lesions visible in all patients and shown to increase over time for patient 7. Loss of autofluorescence corresponding to atrophy with

speckled hypoautofluorescent spots are visible in patients 5 and 8 on FAF imaging. Loss of outer retina and retinal pigment epithelium (RPE) with outer retinal tubulations was seen on OCT in patients 5, 7, and 8 (yellow arrowhead) and cystic spaces of the outer nuclear layer in patient 5. Hyperpigmented lesions correspond to thickened RPE on OCT as demonstrated in patient 5 (yellow arrowheads). Patient 10 has extensive loss of retina, RPE, and choroid with a serous detachment of remaining retina from underlying residual choroid/sclera.

Figure 3. Electroretinography Features



Full-field electroretinogram (ERG) and pattern electroretinogram (PERG) features are shown for 1 eye of patients 3, 5, and 7 and a normal control. Patient 3 has normal dark-adapted (DA) ERGs to flash strengths of 0.01 and 10.0  $\text{cd/s/m}^{-2}$  (DA 0.01 and DA 10.0) and normal light-adapted (LA) ERGs to a flash strength of 3.0  $\text{cd/s/m}^{-2}$  (LA 3.0 30 Hz and 2 Hz); the PERG P50

component is subnormal. Patient 5 shows mild reduction in the right eye DA ERGs and normal LA ERGs; all left eye responses in that patient were normal. In all other patients, the ERGs were symmetrically abnormal. The ERG abnormalities in patient 7 were stable for a 9-year period, but the PERG shows deterioration of macular function.

termination codons and 1 novel missense mutation (Figure 1). The novel missense mutation, c.613G>A (p.Val205Met), was predicted to be damaging in silico (SIFT<sup>0</sup>; PolyPhen2.1.0). Only 1 other mutation, Arg503His, was a missense mutation that has

been previously reported in 3 affected families.<sup>3,4</sup> Both missense variants arise in codons that are highly conserved across species. Patient 1 was a compound heterozygote; all other patients had homozygote mutations.

## Discussion

This study of *CDH3*-related retinal dystrophy reports detailed phenotyping of patients with molecularly confirmed disease and characterizes the key ophthalmic and systemic features, which confirm the disorder to be progressive. This report may allow improved recognition of this disorder and provide more accurate prognostic information for patients.

The patients all presented in childhood or adolescence with central visual disturbance, sparse scalp hair, and a predominantly macular dystrophy. Most of the previously described patients also presented with reduced VA in childhood except for 1 family in which the eldest child had normal VA at 14 years of age despite visible macular pigmentary change.<sup>4</sup>

Visual acuity in the present series deteriorated over time, except in 1 patient with stable and good VA after 20 years of review and preserved foveal photoreceptors on OCT. Longitudinal data on VA decline have not, to our knowledge, previously been reported, although decreased VA with patient age has been observed.<sup>15</sup> Patient 1 was unusual within this series for having mild structural changes in the macula. Despite this, VA was significantly reduced, indicating that the function of the macula was impaired before the development of visible atrophy. Although most of the previously reported patients had marked macular atrophy encompassing the disc, 1 patient with mild atrophic changes and syndactyl of his left foot has been described.<sup>6</sup> The refractile deposits in patient 7 were much smaller than the expected size of refractile drusen, and no other cause could be elucidated from the patient's medical history.<sup>21</sup> It remains unclear whether these deposits are related to *CDH3* because they have not been observed and reported in any other patient.

Detailed retinal imaging has previously been reported in only 1 patient.<sup>16</sup> That 6-year-old patient had typical features of posterior pole atrophy with early loss of photoreceptors and RPE on OCT. In contrast, 7 patients in this study underwent FAF imaging and 9 underwent OCT. Apart from patient 1 in this series, all patients had marked and confluent hypoautofluorescence on FAF imaging that corresponded to the atrophic region. This region was surrounded by an apparent ring of increased autofluorescence. In general, OCT imaging demonstrated loss of outer retina and RPE and frequent outer retinal tubulations. The posterior pole appears to show atrophy from early childhood. The degree of atrophy within that region progressed with time (based on OCT findings), but the overall area of atrophy (based on FAF imaging) did not appear to increase, although this latter observation was limited by numbers available for analysis.

Bilateral ERG abnormalities were present in 2 of 5 cases and were relatively mild, whereas most had PERG evidence of severe macular dysfunction in keeping with the retinal imaging. The disorder appeared to be largely confined to the posterior pole. Serial ERGs available in 1 patient demonstrated that the full-field ERG abnormalities did not progress with time, but the PERG, a measure of macular function, deteriorated during the same 9-year period. The EOG was normal in the 2 patients with test results, consistent with most previous

reports.<sup>5,12,16</sup> These previous reports have largely focused on ERG and EOG findings, with only 1 report of PERG in HJMD.<sup>12</sup> That patient had very poor vision at age 48 years, an undetectable PERG, and reduced cone-derived ERGs. The ERG findings have otherwise been normal or showed subnormal rod and/or cone responses.<sup>2-6,10,12,14-16</sup> One patient was reported to have severe retinal dysfunction on ERG but without further details.<sup>8</sup>

The most common cause of juvenile-onset macular dystrophy is Stargardt macular dystrophy due to biallelic mutations in *ABCA4* (OMIM 601691).<sup>22</sup> That disorder may present with similar symptoms to *CDH3*-related disease, with central visual disturbance, macular atrophy, and electrophysiologic dysfunction confined to the macula (present in one-third of children with Stargardt disease) or macular and generalized retinal dysfunction usually involving cone and rod systems (found in the other two-thirds).<sup>23</sup> Not all patients with Stargardt disease, particularly children, have the distinctive yellow-white flecks at presentation. Patients with HJMD may initially be misdiagnosed with Stargardt disease, but the 2 disorders can be distinguished most readily by examination of the scalp hair. In addition, the peripapillary region is classically but not universally spared in *ABCA4* retinopathy, and the macular atrophy observed in children with Stargardt disease is much less extensive.<sup>24</sup>

*CDH3* encodes P-cadherin, a member of the cadherin transmembrane protein family that forms a major component of adherens junctions important in cell-to-cell interactions, including cell adhesion, cell signaling, and the formation of other membrane structures such as desmosomes.<sup>25,26</sup> A total of 25 mutations in *CDH3* have been reported, including those from this study—7 missense and 2 splice-site mutations—with the rest being premature termination codons (Figure 4 and eTable 2 in the Supplement). All but one of the premature termination codons identified would be predicted to trigger nonsense-mediated decay and lead to haploinsufficiency; the exception, p.G786Afs\*7, arises after the predicted cutoff for nonsense-mediated decay.<sup>27</sup> Patient 8, homozygous for this variant, had onset of visual symptoms later than all other patients in this series but otherwise had a similar retinal phenotype. Four of the 7 missense variants were associated with EEMS, which may indicate that abnormally produced protein has a particularly detrimental effect on limb development.

P-cadherin regulates the development of hair, limbs, and the RPE, as demonstrated by upregulation of its expression in these key locations in mouse embryo studies.<sup>7</sup> Tissue development may be controlled by the affinity of tissue-specific cadherin and their expression levels at certain points in embryogenesis.<sup>28</sup> N-cadherin expression is turned off and P-cadherin expression is turned on as RPE differentiation commences.<sup>29</sup> P-cadherin is not expressed in the neuroretina.<sup>7,29</sup> This finding suggests that photoreceptor loss in *CDH3*-related macular dystrophy is secondary to P-cadherin dysfunction in the RPE. Cadherin proteins are characterized by extracellular, transmembrane, and intracellular domains (Figure 4). The 5 calcium-binding extracellular domains are critical to protein function by mediating dimerization.<sup>30</sup> Reported mutations arise throughout the protein, but all

Figure 4. Schematic Representation of P-Cadherin

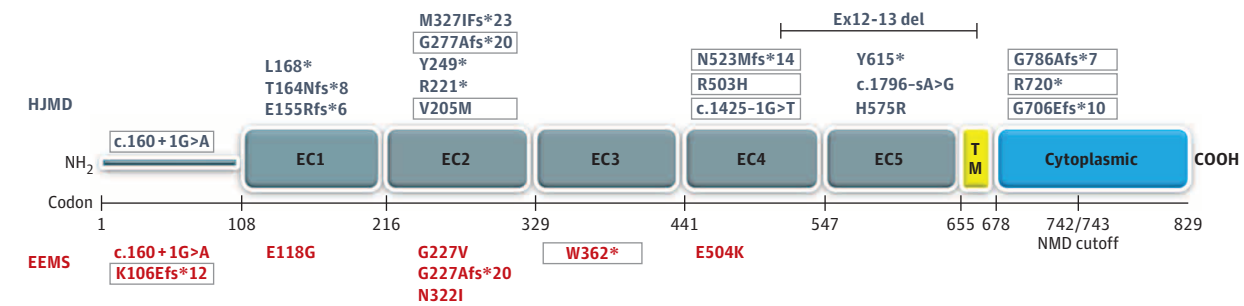


Diagram includes protein domains, previously reported mutations, and mutations from this report (boxed). COOH indicates carboxyl group; EC, extracellular; EEMS, ectodermal dysplasia, ectrodactyly, and macular

dystrophy syndrome; HJMD, hypotrichosis with juvenile macular dystrophy; NH<sub>2</sub>, amine group; NMD, nonsense-mediated decay; and TM, transmembrane.

reported missense variants are found within the extracellular domains, which may indicate that their functional impact is most significant here. The tertiary protein structure for P-cadherin has been experimentally proven using x-ray crystallography for extracellular 1 and 2 domains only.<sup>30</sup>

The site of disease could be primarily RPE with secondary photoreceptor loss. Consistent with this possibility, protein expression in animal models has been located to RPE and not retina.<sup>7,29</sup> In humans, *CDH3* messenger RNA has been identified in expressed sequence tags from RPE.<sup>31</sup> Evidence from the OCT data in the present series suggests that the outer retina and photoreceptors do not show atrophy before RPE loss, as would be expected in a primary photoreceptor disorder. The frequently observed outer retinal tubulations are nonspecific findings of disorders such as Stargardt disease and age-related macular degeneration, which have underlying RPE dysfunction with residual photoreceptors forming these characteristic circular structures.<sup>32</sup> Normal results of EOG studies in 2 patients suggest that HJMD is not a disorder of primary RPE dysfunction.

Alternatively, rather than primary RPE dysfunction, the disorder may be one of concurrent RPE and photoreceptor loss as occurs in choroideremia, in which outer retinal tubulations are also frequently present.<sup>33</sup> Why the retina and RPE in the posterior pole are particularly predisposed to degeneration compared with elsewhere is not clear. The macula is the region of highest cone density and has a higher metabolic demand than the rest of the retina owing to increased phototransduction.<sup>34</sup> This process necessitates an increased demand on the RPE for digestion of shed photoreceptor outer disc membranes, which may be sufficient to compromise the already abnormal RPE cell function and may lead to an accumulation of toxic deposits.<sup>35</sup> In addition, the Bruch

membrane is thinner in the macula than elsewhere in the retina, which may increase susceptibility to damage. Further understanding of *CDH3* protein function in the retina and RPE is ultimately needed to define the location and mechanism of disease.

Although HJMD and EEMS are considered allelic disorders, they may be better considered as part of a phenotypic spectrum in which all patients have hypotrichosis and macular dystrophy with variable additional limb and ectodermal anomalies.<sup>14</sup> The same variant may be associated with a variable phenotype. For example, the variant p.G277Afs\*20 has been associated with HJMD and EEMS in the homozygous state (Figure 3).<sup>4,13</sup> Patient 10 in this report, who had no limb or ectodermal abnormalities, was found to be homozygous for c.160 + 1G>A. This variant has been reported once in a compound heterozygous patient in conjunction with a missense change p.E504K.<sup>6</sup> The reported patient had syndactyly of left foot, although mild, which suggests an EEMS phenotype. Only 3 other variants have been reported in EEMS, all missense changes. Reported limb anomalies include severe split hand or foot malformations, but these may be subtle, such as a single nail dysplasia, and should be specifically looked for in patients presenting with HJMD.<sup>7,14</sup>

## Conclusions

Based on symptoms, visual function, retinal imaging, and electrophysiologic characteristics, *CDH3*-related disease appears to be centrally progressive with preserved peripheral function. The characteristic features, with marked macular dysfunction in childhood associated with thin, sparse hair, are readily recognizable and can aid diagnosis.

### ARTICLE INFORMATION

**Submitted for Publication:** January 25, 2016; final revision received April 26, 2016; accepted May 15, 2016.

**Published Online:** July 7, 2016.

doi:10.1001/jamaophthalmol.2016.2089.

**Author Contributions:** Drs Khan and Webster contributed equally to this research. Dr Hull had full access to all of the data in this study and takes responsibility for the integrity of the data and the accuracy of the data analysis.  
*Study concept and design:* Hull, Michaelides, Khan, Webster.

*Acquisition, analysis, or interpretation of data:* Hull, Arno, Robson, Broadgate, Plagnol, McKibbin, Halford, Holder, Moore, Khan, Webster.  
*Drafting of the manuscript:* Hull, Plagnol, Michaelides, Khan.  
*Critical revision of the manuscript for important intellectual content:* Hull, Arno, Robson, Broadgate, McKibbin, Halford, Michaelides, Holder, Moore,



Khan, Webster.

*Statistical analysis:* Plagnol.

*Obtained funding:* Moore, Webster.

*Administrative, technical, or material support:* Arno, Robson, Broadgate, Holder, Khan, Webster.  
*Study supervision:* Webster.

**Conflict of Interest Disclosures:** All authors have completed and submitted the ICMJE Form for Disclosure of Potential Conflicts of Interest and none were reported.

**Funding/Support:** This study was supported by the National Institute for Health Research and Biomedical Research Centre at Moorfields Eye Hospital, grant BRC2\_003 from the UCL Institute of Ophthalmology, grants 1318 and 1801 from Fight For Sight, grant ST1109B from Moorfields Eye Hospital Special Trustees, a Career Development Award from Foundation Fighting Blindness (Dr Michaelides), Rosetrees Trust, and unrestricted funding from Research to Prevent Blindness USA (Department of Ophthalmology, University of California, San Francisco).

**Role of the Funder/Sponsor:** The funding sources had no role in the design and conduct of the study; collection, management, analysis, and interpretation of the data; preparation, review, or approval of the manuscript; and decision to submit the manuscript for publication.

**Additional Contributions:** Klaus Rohrschneider, FEBO, Heidelberg University Eye Clinic, Heidelberg, Germany, conducted clinical examination and investigation of 1 patient and made the diagnosis, for which he received no additional compensation.

## REFERENCES

- Wagner H. Maculaaffektion, vergesellschaftet mit Haarabnormität von Lanugotypus, beide vielleicht angeboren bei zwei Geschwistern. *Albrecht Von Graefes Arch Ophthalmol.* 1935;134:74-81.
- Sprecher E, Bergman R, Richard G, et al. Hypotrichosis with juvenile macular dystrophy is caused by a mutation in *CDH3*, encoding P-cadherin. *Nat Genet.* 2001;29(2):134-136.
- Indelman M, Bergman R, Lurie R, et al. A missense mutation in *CDH3*, encoding P-cadherin, causes hypotrichosis with juvenile macular dystrophy. *J Invest Dermatol.* 2002;119(5):1210-1213.
- Indelman M, Hamel CP, Bergman R, et al. Phenotypic diversity and mutation spectrum in hypotrichosis with juvenile macular dystrophy. *J Invest Dermatol.* 2003;121(5):1217-1220.
- Indelman M, Leibur R, Jammal A, Bergman R, Sprecher E. Molecular basis of hypotrichosis with juvenile macular dystrophy in two siblings. *Br J Dermatol.* 2005;153(3):635-638.
- Indelman M, Eason J, Hummel M, et al. Novel *CDH3* mutations in hypotrichosis with juvenile macular dystrophy. *Clin Exp Dermatol.* 2007;32(2):191-196.
- Shimomura Y, Wajid M, Shapiro L, Christiano AM. P-cadherin is a p63 target gene with a crucial role in the developing human limb bud and hair follicle. *Development.* 2008;135(4):743-753.
- Jelani M, Salman Chishti M, Ahmad W. A novel splice-site mutation in the *CDH3* gene in hypotrichosis with juvenile macular dystrophy. *Clin Exp Dermatol.* 2009;34(1):68-73.
- Shimomura Y, Wajid M, Kurban M, Christiano AM. Splice site mutations in the P-cadherin gene underlie hypotrichosis with juvenile macular dystrophy. *Dermatology.* 2010;220(3):208-212.
- Kamran-ul-Hassan Naqvi S, Azeem Z, Ali G, Ahmad W. A novel splice-acceptor site mutation in *CDH3* gene in a consanguineous family exhibiting hypotrichosis with juvenile macular dystrophy. *Arch Dermatol Res.* 2010;302(9):701-703.
- Avitan-Hersh E, Indelman M, Khamaysi Z, Leibur R, Bergman R. A novel nonsense *CDH3* mutation in hypotrichosis with juvenile macular dystrophy. *Int J Dermatol.* 2012;51(3):325-327.
- Halford S, Holt R, Németh AH, Downes SM. Homozygous deletion in *CDH3* and hypotrichosis with juvenile macular dystrophy. *Arch Ophthalmol.* 2012;130(11):1490-1492.
- Kjaer KW, Hansen L, Schwabe GC, et al. Distinct *CDH3* mutations cause ectodermal dysplasia, ectrodactyly, macular dystrophy (EEM syndrome). *J Med Genet.* 2005;42(4):292-298.
- Basel-Vanagaite L, Pasmanik-Chor M, Lurie R, Yeheskel A, Kjaer KW. *CDH3*-related syndromes: report on a new mutation and overview of the genotype-phenotype correlations. *Mol Syndromol.* 2010;1(5):223-230.
- Leibu R, Jermans A, Hatim G, Miller B, Sprecher E, Perlman I. Hypotrichosis with juvenile macular dystrophy: clinical and electrophysiological assessment of visual function. *Ophthalmology.* 2006;113(5):841-847.e3.
- Mason JO III, Patel SA. A case of hypotrichosis with juvenile macular dystrophy. *Retin Cases Brief Rep.* 2015;9(2):164-167.
- World Medical Association. World Medical Association Declaration of Helsinki: ethical principles for medical research involving human subjects. *JAMA.* 2013;310(20):2191-2194. doi:10.1001/jama.2013.281053.
- McCulloch DL, Marmor MF, Brigell MG, et al. ISCEV standard for full-field clinical electroretinography (2015 update). *Doc Ophthalmol.* 2015;130(1):1-12.
- Bach M, Brigell MG, Hawlina M, et al. ISCEV standard for clinical pattern electroretinography (PERG): 2012 update. *Doc Ophthalmol.* 2013;126(1):1-7.
- Glöckle N, Kohl S, Mohr J, et al. Panel-based next generation sequencing as a reliable and efficient technique to detect mutations in unselected patients with retinal dystrophies. *Eur J Hum Genet.* 2014;22(1):99-104.
- Suzuki M, Curcio CA, Mullins RF, Spaide RF. Refractile drusen: clinical imaging and candidate histology. *Retina.* 2015;35(5):859-865.
- Allikmets R. A photoreceptor cell-specific ATP-binding transporter gene (*ABCR*) is mutated in recessive Stargardt macular dystrophy. *Nat Genet.* 1997;17(1):122.
- Fujinami K, Zernant J, Chana RK, et al. Clinical and molecular characteristics of childhood-onset Stargardt disease. *Ophthalmology.* 2015;122(2):326-334.
- Hwang JC, Zernant J, Allikmets R, Barile GR, Chang S, Smith RT. Peripapillary atrophy in Stargardt disease. *Retina.* 2009;29(2):181-186.
- Gumbiner BM. Cell adhesion: the molecular basis of tissue architecture and morphogenesis. *Cell.* 1996;84(3):345-357.
- Huen AC, Park JK, Godsel LM, et al. Intermediate filament-membrane attachments function synergistically with actin-dependent contacts to regulate intercellular adhesive strength. *J Cell Biol.* 2002;159(6):1005-1017.
- Lejeune F, Maquat LE. Mechanistic links between nonsense-mediated mRNA decay and pre-mRNA splicing in mammalian cells. *Curr Opin Cell Biol.* 2005;17(3):309-315.
- Duguay D, Foty RA, Steinberg MS. Cadherin-mediated cell adhesion and tissue segregation: qualitative and quantitative determinants. *Dev Biol.* 2003;253(2):309-323.
- Xu L, Overbeek PA, Reneker LW. Systematic analysis of E-, N- and P-cadherin expression in mouse eye development. *Exp Eye Res.* 2002;74(6):753-760.
- Dalle Vedove A, Lucarelli AP, Nardone V, Matino A, Parisini E. The x-ray structure of human P-cadherin EC1-EC2 in a closed conformation provides insight into the type I cadherin dimerization pathway. *Acta Crystallogr F Struct Biol Commun.* 2015;71(pt 4):371-380.
- Boguski MS, Lowe TM, Tolstoshev CM. dbEST: database for "expressed sequence tags." *Nat Genet.* 1993;4(4):332-333.
- Goldberg NR, Greenberg JP, Laud K, Tsang S, Freund KB. Outer retinal tubulation in degenerative retinal disorders. *Retina.* 2013;33(9):1871-1876.
- Roosing S, Collin RW, den Hollander AI, Cremers FP, Siemiatkowska AM. Prenylation defects in inherited retinal diseases. *J Med Genet.* 2014;51(3):143-151.
- Khandhadia S, Lotery A. Oxidation and age-related macular degeneration: insights from molecular biology. *Expert Rev Mol Med.* 2010;12:e34.
- Volland S, Esteve-Rudd J, Hoo J, Yee C, Williams DS. A comparison of some organizational characteristics of the mouse central retina and the human macula. *PLoS One.* 2015;10(4):e0125631.